NASA TECHNICAL NOTE

NASA TN D-3173

NASA TN D-3173

EQUILIBRIUM SHAPE OF AN ARRAY OF LONG ELASTIC STRUCTURAL MEMBERS IN CIRCULAR ORBIT

by Thomas W. Flatley

Goddard Space Flight Center

Greenbelt, Md.

NATIONAL AERONAUTICS AND SPACE ADMINISTRATION • WASHINGTON, D. C. • MARCH 1966

NASA TN D-3173

EQUILIBRIUM SHAPE OF AN ARRAY OF LONG ELASTIC STRUCTURAL MEMBERS IN CIRCULAR ORBIT

By Thomas W. Flatley

Goddard Space Flight Center
Greenbelt, Md.

NATIONAL AERONAUTICS AND SPACE ADMINISTRATION

For sale by the Clearinghouse for Federal Scientific and Technical Information
Springfield, Virginia 22151 – Price $0.30

ABSTRACT

19589

The equilibrium shape of an array of long elastic structural members in circular orbit under the influence of gravitational, inertial, and solar pressure forces and thermal bending is considered. Appropriate nonlinear differential equations governing the deflection of thin beams in the orbital environment are derived, and a method of solution exploiting the repetitive operation and oscilloscopic display capability of some analog computers is described. The analysis is then applied to a Radio Astronomy Explorer satellite design with four coplanar booms extending as cantilever beams from a central body, and arranged so as to act simultaneously as antennas and gravity-gradient attitude control rods.

Author

CONTENTS

EQUILIBRIUM SHAPE OF AN ARRAY OF LONG ELASTIC STRUCTURAL MEMBERS IN CIRCULAR ORBIT

by
Thomas W. Flatley
Goddard Space Flight Center

INTRODUCTION

The present analysis was undertaken in support of preliminary planning for a radio astronomy satellite which will study galactic electromagnetic radiation in the 1- to 10-megacycle range; this radiation is shielded from ground-based radio telescopes by the atmosphere of the earth.

The configuration considered here is one which has been chosen for initial flights and represents a compromise between antenna requirements and ease of mechanization and control. Basically, it consists of four coplanar booms (Figure 1) extending as cantilever beams from a central body; the booms are arranged so as to act simultaneously as antennas and gravity-gradient control rods.

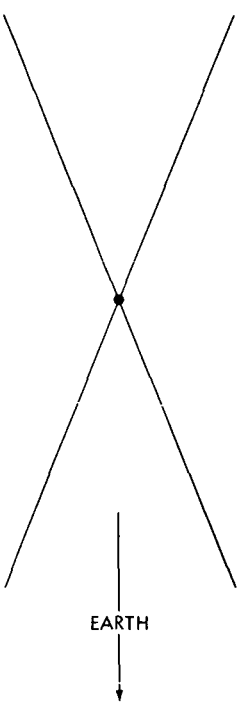

Figure 1—Configuration of four coplanar booms.

When the configuration has been placed in circular orbit, one pair of booms forms a "V" antenna pointing radially outward from the earth and scans a great circle on the celestial sphere once per orbit, while the other pair scans the earth and measures background noise from terrestrial sources. Nodal regression introduces a gradual rotation of the scanning plane, allowing eventual wide coverage of the celestial sphere.

Interpretation of the experimental data will require an accurate knowledge of the antenna pattern at the time of observation and thus an accurate knowledge of the antenna shape. The purpose of this analysis is to provide a first approximation to the equilibrium shape of such a configuration under the influence of gravitational, inertial, and solar pressure forces and thermal bending. Experimentally determined antenna patterns based on the shapes found with various design and orbit parameters would then be an important factor in the selection of actual flight parameters.

The boom lengths (750 to 1000 feet) required by the nature of the experiment and the payload weight limitations of proposed launch vehicles (200 to 300 pounds for preferable orbits) necessitate the use of unusual beams which cannot support their own weight here on earth. Although the loading

that the orbiting array of booms will be exposed to is very small, it is easily sufficient, because of the extreme flexibility of the members, to make this a problem of elastica (the nonlinear deflection of long, thin beams) and a most unusual one.

The problem is essentially reduced to one of static, two-dimensional deflection of a fixed-free cantilever beam when a circular orbit about a spherical earth with ideal gravity-gradient attitude control of the central body is assumed and the sun is taken to be in the plane of the booms. The combined effects of mechanical loading and thermal bending are considered, with the former arising from gravitational, inertial, and solar pressure forces and the latter from a temperature gradient across the boom cross section.

Interesting complications are introduced because most of these disturbances prove to be functions not only of beam station but also of deflection and slope and because the thermal effects do not vanish with the mechanical loading at the free end.

BEAM BENDING ANALYSIS

For any plane curve,

$$\frac{d\theta}{ds} = \frac{1}{r} , \tag{1}$$

where

θ = slope of a line drawn tangent to the curve with respect to some reference line in the plane,

s = length of curve, and

r = radius of curvature.

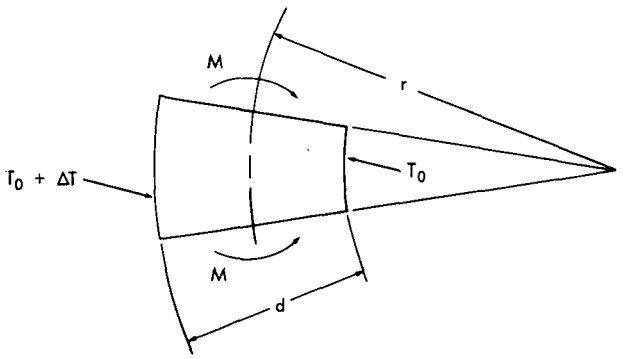

Figure 2—Beam subject to a bending moment and a linear temperature gradient.

Equation 1 becomes the basic differential equation for any planar elastic beam bending if an expression for the radius of curvature can be found.

Consider a section of a beam subject to a bending moment M and a linear temperature gradient $\Delta T/d$ where d is the beam width (Figure 2).

Let Δs be the length of the beam section for the case $M = \Delta T = 0$. Under load, the new

length of the innermost fiber (ℓ_1) is independent of ΔT and will be determined by the compressive strain due to the bending moment according to

$$\begin{aligned} \ell_1 &= \Delta s\,(1 + \text{Strain}) \\ &= \Delta s\,\left[1 + (\text{Stress}/E)\right] \\ &= \Delta s\,\left[1 + \left(\frac{Mc}{I}/E\right)\right] \\ &= \Delta s\,\left(1 - \frac{Md}{2EI}\right), \end{aligned} \tag{2}$$

where

E = modulus of elasticity of beam material,

I = moment of inertia of cross section, and

c = -d/2, distance of fiber from neutral axis.

The new length of the center fiber (ℓ_2) is independent of M and will be determined by the expansion due to the temperature gradient according to

$$\begin{aligned} \ell_2 &= \Delta s\,(1 + \text{Expansion per unit length}) \\ &= \Delta s\left(1 + e\,\frac{\Delta T}{2}\right), \end{aligned} \tag{3}$$

where e is the thermal expansion coefficient of the beam material.

Now, by similar triangles (Figure 3) with $r \gg \Delta s$,

$$\frac{\ell_2}{r} = \frac{\ell_1}{r - \frac{d}{2}}. \tag{4}$$

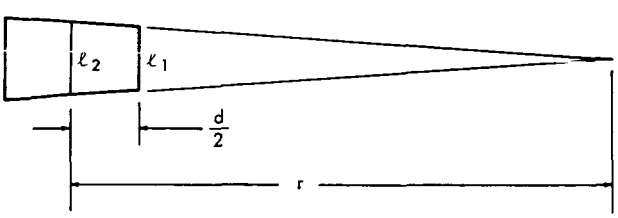

Figure 3—Determination of beam lengths.

When the calculated values of ℓ_1 and ℓ_2 from Equations 2 and 3 are substituted in Equation 4,

$$\Delta s\left(1 + e\,\frac{\Delta T}{2}\right)\left(r - \frac{d}{2}\right) = \Delta s\left(1 - \frac{Md}{2EI}\right) r,$$

or

$$\left(1 + e\,\frac{\Delta T}{2}\right)\left(1 - \frac{d}{2r}\right) = \left(1 - \frac{Md}{2EI}\right). \tag{5}$$

For values of $e\ \Delta T/2$ and $d/2r \ll 1$,

$$e\,\frac{\Delta T}{2} - \frac{d}{2r} \approx -\frac{Md}{2EI}$$

and

$$\frac{1}{r} \approx \frac{e\,\Delta T}{d} + \frac{M}{EI} . \tag{6}$$

Substituting Equation 6 in Equation 1 and adopting the convention that values of $r > 0$ cause the slope to decrease give

$$\frac{d\theta}{ds} = -\frac{M}{EI} - \frac{e\,\Delta T}{d} . \tag{7}$$

This, then, is the basic differential equation for the elastic deflection of a beam under the combined influence of mechanical loading and thermal bending.

A rotating coordinate system (Figure 4a) with origin at the center of mass of a satellite in circular orbit is now defined. The positive x-axis is directed outward along the local vertical, and the positive y-axis is in the direction of the satellite velocity vector $\vec{v}$. Consider both an array of booms and the sun in the x-y or orbital plane, with the beam slope θ and the sun location α measured with respect to the x-axis (Figure 4b).

Now, ΔT will be a function of the angle of incidence of the sun's rays and will range from some maximum positive value for the case $\alpha - \theta = \pi/2$ to a maximum negative value for $\alpha - \theta = -\pi/2$. If the functional relationship $\Delta T = \Delta T_{max} \sin(\alpha - \theta)$ is assumed, Equation 7 becomes

$$\frac{d\theta}{ds} = -\frac{M}{EI} - \frac{e\,\Delta T_{max}}{d} \sin(\alpha - \theta) . \tag{8}$$

The temperature ΔT_{max} must be determined by thermodynamic analysis and will depend on factors such as the physical dimensions of the cross section, the type and reflectivity of the surface coatings used, and the thermal conductivity of the materials. In practical applications of long thin booms it is a very critical item, and extensive efforts are being devoted to minimize ΔT_{max} and thus limit thermal deflections.

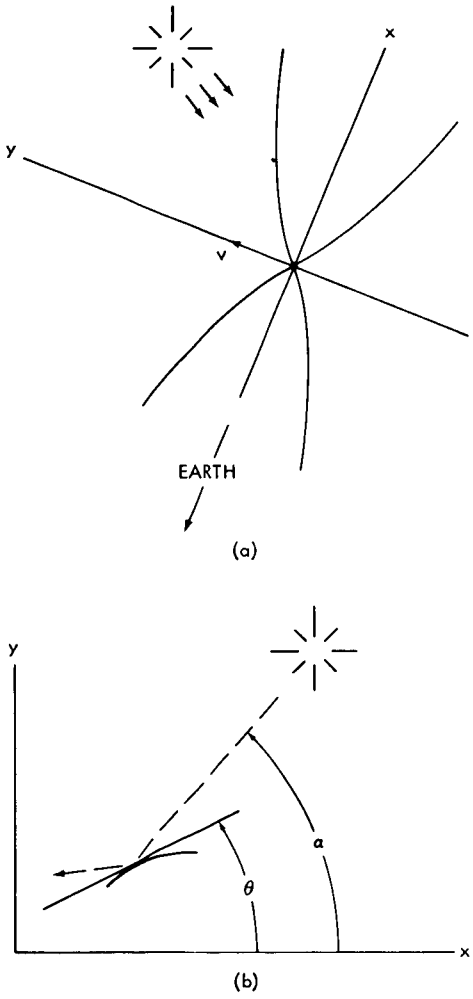

Figure 4—Sketch of coordinates. (a) Rotating coordinate system with origin at center of mass of a satellite in circular orbit. (b) Measurement of beam slope θ and sun location α.

In order to find the bending moment M, consideration must be given to the mechanical loading to which the beam is exposed. In the present problem the loading is purely distributed and arises from solar pressure, gravitational, and inertial forces.

It is now necessary to determine this mechanical loading and then to consider how it and the bending moment are related in the case of large deflections. The geometry of the beam cross section must be specified before solar pressure effects can be considered. In the present case, the beam cross section will be assumed to be circular (Figure 5). For $\alpha > \theta$, the upper half of the beam section will be illuminated as seen in Figure 6.

Consider an element of illuminated area $(d/2)\, d\phi\, ds$. The unit vector normal to this area is

$$\vec{n} = \begin{pmatrix} -\cos\phi & \sin\theta \\ \cos\phi & \cos\theta \\ \sin\phi \end{pmatrix} .$$

A unit vector parallel to the sun's rays is

$$\vec{s} = \begin{pmatrix} \cos\alpha \\ \sin\alpha \\ 0 \end{pmatrix} .$$

The effective area exposed to the solar flux is given by

$$\begin{aligned} dA_{eff} &= \frac{d}{2} (\vec{n} \cdot \vec{s})\, d\phi\, ds \\ &= \frac{d}{2} \cos\phi (\sin\alpha \cos\theta - \cos\alpha \sin\theta)\, d\phi\, ds \\ &= \frac{d}{2} \cos\phi \sin(\alpha - \theta)\, d\phi\, ds \quad . \end{aligned} \tag{9}$$

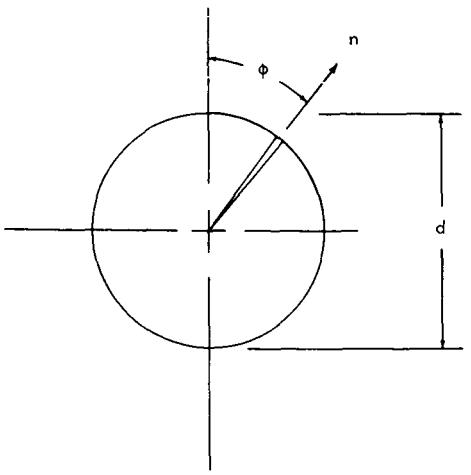

Figure 5—Geometry of a beam cross section.

If this area is to be always positive

$$dA_{eff} = \frac{d}{2} \cos\phi \, |\sin(\alpha - \theta)| \, d\phi\, ds \quad . \tag{10}$$

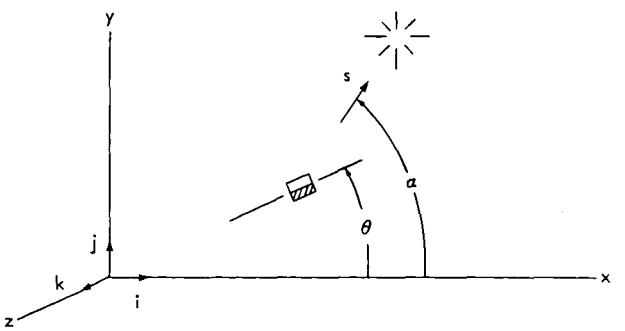

Figure 6—Illumination of a beam section when $\alpha > \theta$.

When 100-percent spectral and total reflection of the sun's rays is assumed, the force exerted on the element of area is normal to the surface and is given by

$$dF = 2p_o (\vec{n} \cdot \vec{s})\, dA_{eff} , \tag{11}$$

where p_o is the solar pressure in the vicinity of the earth.

From symmetry, it is seen that the only component of this force which contributes to the net load on the beam is $\cos\phi\, dF$. In order to find the normal load per unit length due to solar radiation, we integrate over the illuminated portion of the beam section (Figure 7):

$$\begin{aligned} W_{sp} &= \frac{2\int_0^{\pi/2} \cos\phi\, dF}{ds} \\ &= \frac{4p_o \sin(\alpha-\theta)}{ds} \int_0^{\pi/2} \cos^2\phi\, dA_{eff} \\ &= 2p_o\, d \sin(\alpha-\theta)\, |\sin(\alpha-\theta)| \int_0^{\pi/2} \cos^3\phi\, d\phi \\ &= \frac{4}{3} p_o\, d \sin(\alpha-\theta)\, |\sin(\alpha-\theta)| \quad . \end{aligned} \tag{12}$$

In order to determine the gravitational and inertial loading, consider a location (x, y) on the beam which determines a position vector $\vec{R}$ (Figure 8). Under the constraints listed previously in the introduction, the only inertial loading will arise from the centripetal acceleration and will be

$$\vec{u}_1 = \rho\omega^2 \vec{R} , \tag{13}$$

where ρ is the linear mass density.

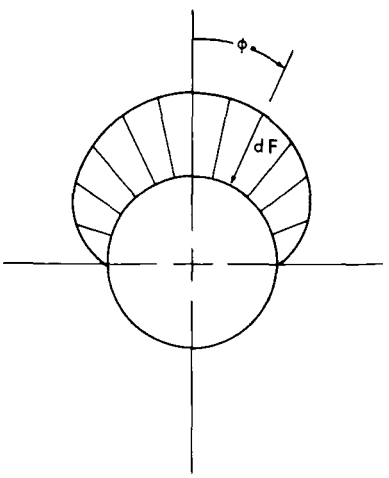

Figure 7—Solar pressure force on a circular beam cross section with upper half illuminated.

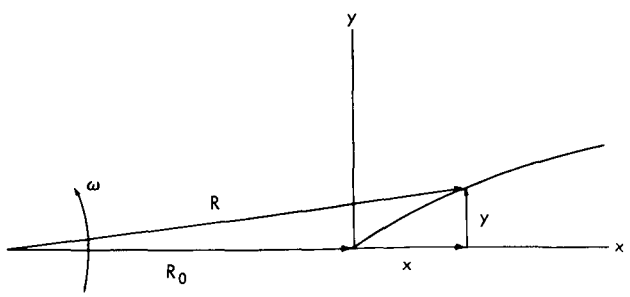

Figure 8—Coordinate system used to determine gravitational and inertial loading.

The gravitational loading will be

$$\vec{u}_2 = -\frac{GM\rho}{R^3}\vec{R}\ , \tag{14}$$

where GM is the earth's gravity constant. At the center of mass (0, 0), $\vec{u}_1 + \vec{u}_2 = 0$, so we can write

$$\rho\omega^2 \vec{R}_0 = \frac{GM\rho}{R_0^3}\vec{R}_0\ ,$$

from which

$$GM = R_0^3\,\omega^2\ . \tag{15}$$

Thus, in general,

$$\vec{u}_1 + \vec{u}_2 = \rho\omega^2\left(1 - \frac{R_0^3}{R^3}\right)\vec{R}\ . \tag{16}$$

Since

$$R^2 = (R_0 + x)^2 + y^2\ ,$$

$$\frac{R_0^3}{R^3} = R_0^3\left(R_0^2 + 2R_0 x + x^2 + y^2\right)^{-3/2}\ , \tag{17}$$

and, for $x, y \ll R_0$,

$$\frac{R_0^3}{R^3} \simeq R_0^3\left(R_0^2 + 2R_0 x\right)^{-3/2}$$

$$= \left(1 + 2\frac{x}{R_0}\right)^{-3/2}$$

$$\simeq 1 - 3\frac{x}{R_0}\ . \tag{18}$$

Therefore,

$$\vec{u}_1 + \vec{u}_2 \simeq \rho\omega^2\left(\frac{3x}{R_0}\right)\left(\vec{R}_0 + \vec{x} + \vec{y}\right)\ ,$$

$$\simeq 3\rho\omega^2 x\frac{\vec{R}_0}{R_0}\ . \tag{19}$$

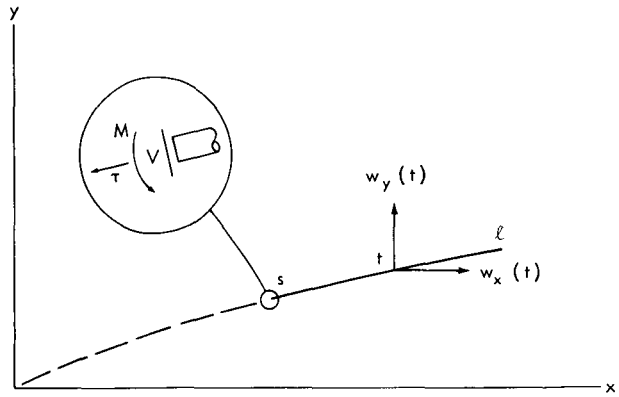

Figure 9—Free-body diagram with coordinate system used to determine mechanical loading and bending moment.

The load per unit length due to the combined gravitational and inertial forces, the "gravity gradient" loading, is thus

$$W_{GG} = 3\rho\omega^2 x \ , \tag{20}$$

parallel to the x-axis.

The relationship between the mechanical loading and the bending moment can be found from the free-body diagram below (Figure 9). Let the total reaction at point s consist of a tension force τ, a shear force V, and a bending moment M. For static equilibrium, it is necessary that

$$M(s) + \int_s^\ell \left\{ \left[x(t) - x(s)\right] W_y(t) - \left[y(t) - y(s)\right] W_x(t) \right\} dt = 0 \tag{21a}$$

$$V\cos\theta(s) - \tau\sin\theta(s) + \int_s^\ell W_y(t)\,dt = 0 \ , \tag{21b}$$

and

$$-V\sin\theta(s) - \tau\cos\theta(s) + \int_s^\ell W_x(t)\,dt = 0 \ . \tag{21c}$$

Differentiating Equation 21a with respect to s, produces

$$\frac{dM(s)}{ds} = \frac{dx(s)}{ds}\int_s^\ell W_y(t)\,dt - \frac{dy(s)}{ds}\int_s^\ell W_x(t)\,dt \ . \tag{22}$$

When Equations 21b and 21c are combined and τ is eliminated ($dx/ds = \cos\theta$ and $dy/ds = \sin\theta$ in the following equations),

$$\begin{aligned} V &= -\cos\theta(s)\int_s^\ell W_y(t)\,dt + \sin\theta(s)\int_s^\ell W_x(t)\,dt \\ &= -\frac{dx(s)}{ds}\int_s^\ell W_y(t)\,dt + \frac{dy(s)}{ds}\int_s^\ell w_x(t)\,dt \\ &= -\frac{dM}{ds} \ . \end{aligned} \tag{23}$$

When Equations 21b and 21c are combined and V is eliminated,

$$\tau = \sin\theta(s) \int_s^{\ell} W_y(t)\,dt + \cos\theta(s) \int_s^{\ell} W_x(t)\,dt \ . \tag{24}$$

By differentiating the expressions for V and τ,

$$\frac{dV}{ds} = \sin\theta(s) \frac{d\theta}{ds} \int_s^{\ell} W_y(t)\,dt + W_y(s)\cos\theta(s)$$

$$+ \cos\theta(s) \frac{d\theta}{ds} \int_s^{\ell} W_x(t)\,dt - W_x(s)\sin\theta(s)$$

$$= \tau \frac{d\theta}{ds} + W_y(s)\cos\theta(s) - W_x(s)\sin\theta(s) \tag{25}$$

and

$$\frac{d\tau}{ds} = \cos\theta(s) \frac{d\theta}{ds} \int_s^{\ell} W_y(t)\,dt - W_y(s)\sin\theta(s)$$

$$- \sin\theta(s) \frac{d\theta}{ds} \int_s^{\ell} W_x(t)\,dt - W_x(s)\cos\theta(s)$$

$$= - V \frac{d\theta}{ds} - W_y(s)\sin\theta(s) - W_x(s)\cos\theta(s) \ . \tag{26}$$

Equations 25 and 26 can be written in terms of the normal and tangential components of the loading (see Figure 10):

$$\frac{dV}{ds} = - W_n + \tau \frac{d\theta}{ds} \tag{27}$$

$$\frac{d\tau}{ds} = - W_t - V \frac{d\theta}{ds} \tag{28}$$

In the present problem,

$$W_n = W_{sp} + W_{gg}\sin\theta \ , \tag{29}$$

and

$$W_t = W_{gg}\cos\theta \ , \tag{30}$$

where W_{sp} and W_{gg} (see Figure 11) have the values given in

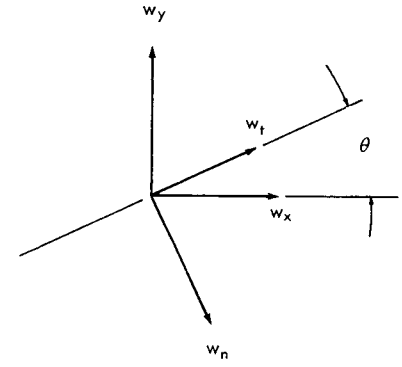

Figure 10—Normal and tangential components of loading.

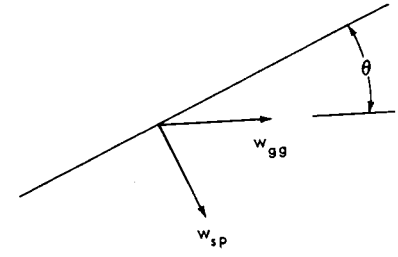

Figure 11—Components due to solar and gravitational forces.

Equations 12 and 20. The set of differential equations governing the deflection of the booms then becomes

$$\left.\begin{aligned} \frac{d\theta}{ds} &= -\frac{M}{EI} - \frac{e\,\Delta T_{max}}{d}\sin(\alpha-\theta) \\ \frac{dM}{ds} &= -V \\ \frac{dV}{ds} &= -\frac{4}{3}p_o d\sin(\alpha-\theta)\,|\sin(\alpha-\theta)| - 3\rho\omega^2 x\sin\theta + \tau\frac{d\theta}{ds} \\ \frac{d\tau}{ds} &= -3\rho\omega^2 x\cos\theta - V\frac{d\theta}{ds}\ , \end{aligned}\right\} \qquad (31)$$

where

$$x = \int_0^s \cos\theta\, ds\ .$$

SOLUTION OF EQUATIONS

Because of the formidable nonlinearity and the coupled nature of the system of differential equations derived, a machine solution was sought. An analog computer with repetitive-operation capability and oscilloscopic display of several problem variables was found to be an ideal tool.

An analog computer is a time-integrating machine, so that a suitable change of variable, such as

$$s = kt$$

and

$$\frac{d}{ds}(\ ) = \frac{1}{k}\frac{d}{dt}(\ ) = \frac{(\dot{\ })}{k}\ ,$$

is a required preliminary step. In addition, problem variables are represented by voltages on the computer and must be scaled so that working voltages are of convenient magnitudes. For a computer designed to operate in the range of ±10 volts, for instance, the quantity $[10\sin\theta]$ would be more useful than $[\sin\theta]$ (the brackets indicate "computer variables"). Wherever $\sin\theta$ appears in an

equation, it is therefore replaced by $1/10\,[10 \sin\theta]$. Similarly, it is necessary to substitute $1/a_i[a_i F_i(t)]$, where a_i is a suitable "scale factor," for other functions $F_i(t)$.

For the sake of clarity in discussing the general method of solution for the system of equations, all constant quantities will be ignored, including those introduced by the change of variable and scaling. For constant values E, I, e, ΔT_{max}, d, p_o, ρ, and ω, consider the following set of equations derived from Equations 31:

$$\left.\begin{aligned} \dot{\theta} &= -M - \sin(\alpha-\theta) \\ \dot{M} &= -V \\ \dot{V} &= -\sin(\alpha-\theta)\,|\sin(\alpha-\theta)| - x\sin\theta + \tau\dot{\theta} \\ \dot{\tau} &= -x\cos\theta - V\dot{\theta} \\ \dot{x} &= \cos\theta \end{aligned}\right\} \qquad (32)$$

The symbol for, and the result of the operation of an analog computer integrator are shown in Figure 12 (note the sign inversion). A set of five integrators, one for each of the differential equations involved, is shown in Figure 13. Here θ can be used to generate $\sin\theta$, $\cos\theta$, $\sin(\alpha-\theta)$, and $|\sin(\alpha-\theta)|$ through the use of function generators, summers, and comparators (see Figure 14). This is the equipment necessary for computing all of the variables appearing in Equations 32, so, with the additional help of a few multipliers (Figure 14d), the complete computer circuit shown in Figure 15 can now be developed.

The analog computer is by nature an "initial-condition" type of machine and requires, in this case, the initial values θ_o, M_o, V_o, τ_o, and x_o as inputs. θ_o is merely the initial slope of the beam and presents no problem, and, $x_o = 0$. The boundary conditions associated with the other variables are imposed at the free end of the beam, however, and they arise from the vanishing of mechanical loading at $s = \ell$. It is thus necessary that

$$M\left(\frac{\ell}{k}\right) = V\left(\frac{\ell}{k}\right) = \tau\left(\frac{\ell}{k}\right) = 0 \qquad (33)$$

and the initial values of these variables are not known.

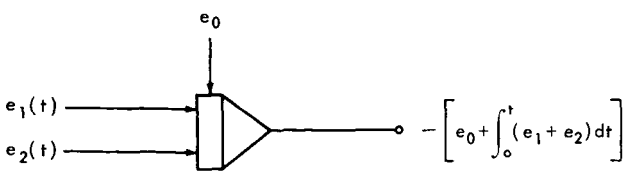

Figure 12—Analog computer integrator.

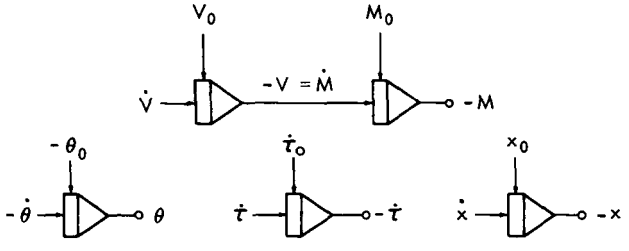

Figure 13—Integrators for Equations 32.

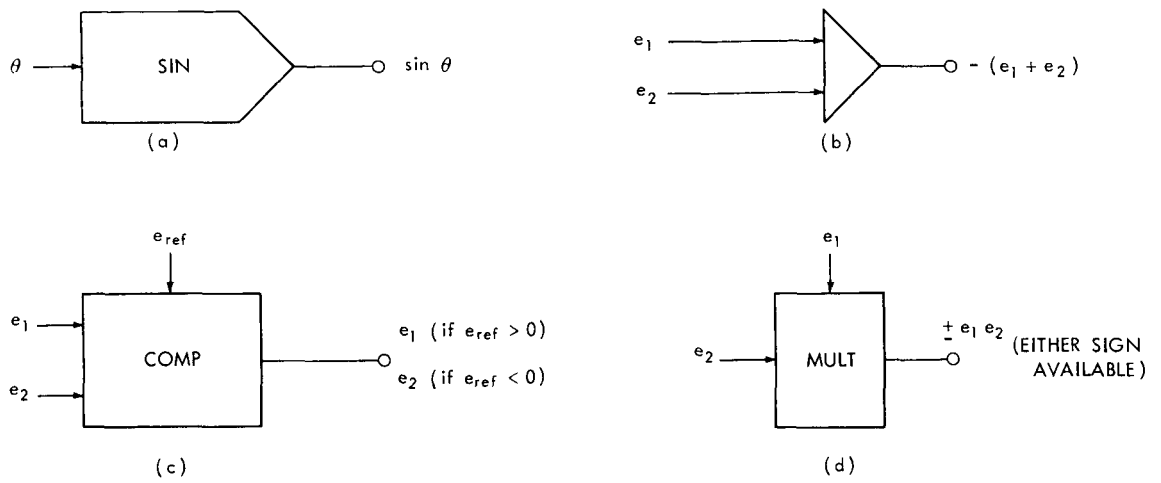

Figure 14—Equipment necessary to compute all variables in Equations 32. (a) Function generator; (b) Summer; (c) Comparator (if $e_1 = e_{ref}$ and $e_2 = -e_1$, then Output = $|e_1|$) (d) Multiplier.

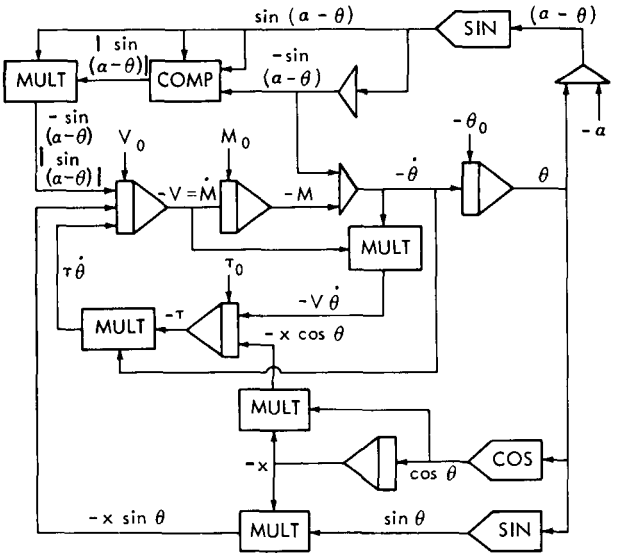

Figure 15—Diagram of the complete computer circuit.

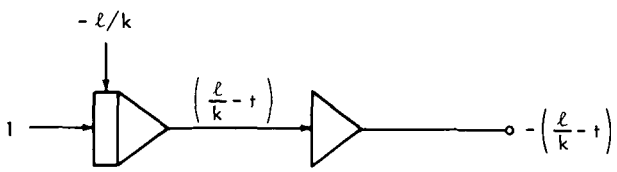

Figure 16—Computation of ± (ℓ/k - t).

Some analog computers have a repetitive operation capability and a built-in multichannel oscilloscope. In its REP-OP mode, the computer rapidly and repeatedly solves a set of equations with the start of each solution triggering the sweep on the scope. The continuous behavior of the variables as functions of time can be displayed by feeding several variables into the oscilloscope. This unique capability was used very successfully in the solution of this problem.

Initial conditions are controlled by potentiometers which can be adjusted while the computer operates in its REP-OP mode. Values of M_o, V_o, and τ_o can be estimated and M, V and τ can be displayed on the oscilloscope. Also the quantities $\pm(\ell/k - t)$ (Figure 16) can be computed and fed into the oscilloscope.

With the computer in operation, the oscilloscopic display might appear as shown in Figure 17. At point B the time $t = \ell/k$ so that this point identifies the time corresponding to $s = \ell$, the free end of the beam. The free-end boundary conditions demand that the moment, shear, and tension curves pass through this point. Solving the problem is reduced to adjusting the three unknown initial conditions in such a way as to achieve this.

Practically speaking, an approximate solution is easily obtained. An upper limit for the tension at the fixed end can be simply calculated, so this is used as a starting point for τ_o. Likewise, simplifying assumptions can be used to get approximate values for M_o and V_o. With a little practice, point A can be readily moved about by manipulating M_o and V_o. By alternately forcing point A to coincide with B, and adjusting τ_o so that the τ curve intersects the t-axis at B, the solution may be quickly found.

What has actually been accomplished in thus finding the solution is the determination of the complete set of initial conditions necessary to satisfy all of the boundary conditions of the problem. If the objective is to determine the actual shape of the beam, we must use the normal mode of computer operation, add a calculation of $y(t)$, and rerun the problem with $x(t)$ and $y(t)$ fed into an x-y plotter (Figure 18).

The larger scale of the plotter makes refinement of the solution possible if desired. Accuracy can be improved by plotting out the variables previously displayed on the oscilloscope and by making small changes in the initial conditions. This is generally not required, however, since the resulting shape changes are insignificant.

In general, a separate solution is required for each boom of an array since the sun aspect angle will be different for each, as shown in Figure 19. In a typical case, after the shape of boom 1 has been determined, we can change α to $-\alpha$, solve the same equations, and plot x versus -y to add boom 2 to the array. The manipulations required for the solution for each boom of the four-boom configuration can be obtained from Table 1.

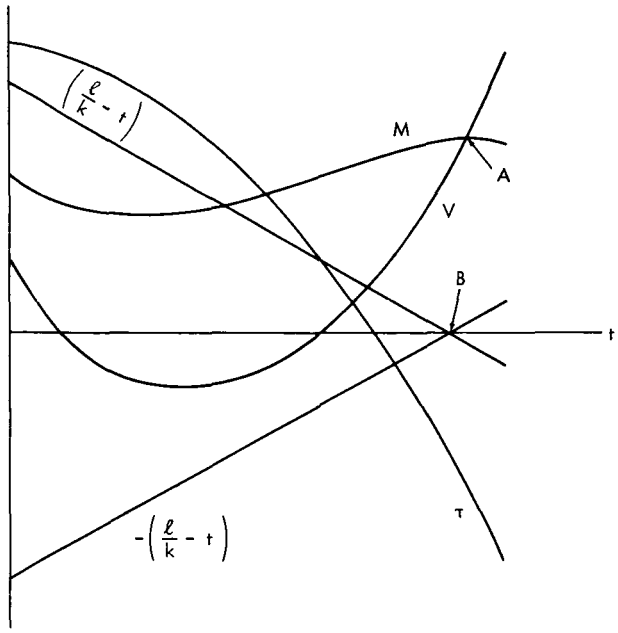

Figure 17—Typical oscilloscopic display of variables.

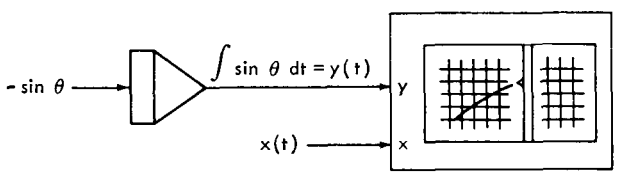

Figure 18—Computer operation to obtain actual shape of beam.

Table 1
Manipulations Required for Determining Various Boom Shapes.

Boom	Value to be substituted for α	Value to be plotted
1	α	x, y
2	$-\alpha$	x, -y
3	$\alpha - \pi$	-x, -y
4	$\pi - \alpha$	-x, y

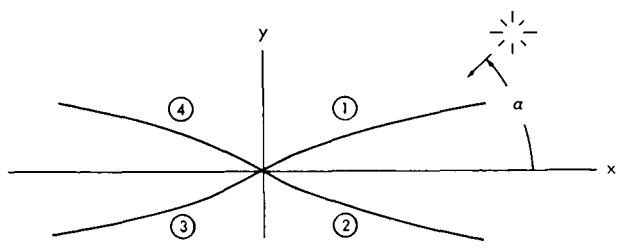

Figure 19—Four-boom configuration.

APPLICATION

The present analysis was developed for, and first applied to, a Radio Astronomy Explorer design which featured hollow, silver-plated beryllium-copper, tubular antennas which are stored on spools during launch and extended in orbit (Figure 20).

Key parameters involved in the study included:

1. Tube diameter = 0.5 inch,
2. Weight = 0.017 pound per foot,
3. Effective stiffness, EI = 10 lb-ft^2,
4. Length = 750 to 1000 feet,
5. "V" half angle = 15° to 30°,
6. Orbital altitude = 2,000 to 10,000 kilometers,
7. Thermal control, ΔT_{max} = 2°F, and
8. Thermal expansion coefficient = 10^{-5} per °F.

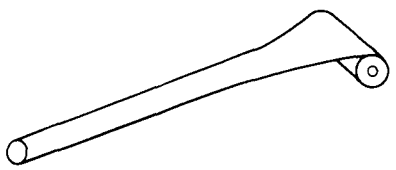

Figure 20—Tubular antenna.

The uselessness of an ordinary linear beam analysis with this set of parameters can readily be seen. In order to demonstrate the inexactness of such an analysis and to indicate the orders of magnitude of the numbers involved in this problem, a calculation by this method is given in Appendix A.

RESULTS

Several series of runs, which involved various combinations of parameters, were conducted, and the results were displayed in different forms. From the various combinations tested, the combination of a 750-foot length, a 22.5-degree half angle and a 6000-kilometer orbital altitude was tentatively selected for flight. This configuration is the only one discussed here and nothing other than comments on the general characteristics of the solutions, the sensitivity to changes in the various parameters, and the presentation of a few typical shapes are given in the present section.

When solar effects are ignored, the gravitational and inertial loadings always tend to close both the upper and lower "V" symmetrically (Figure 21). Since the forces involved are proportional to ω^2, and thus to $1/R_0^3$, the resulting distortion is quite sensitive to altitude.

The introduction of solar effects adds a deflection away from the sun in all cases, with both the solar pressure and the thermal gradient contributing to the deflection. If the sun lies along one

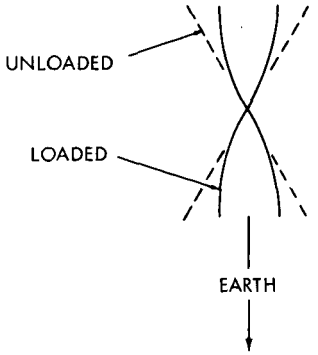

Figure 21—Gravitational and inertial effects on an array of booms.

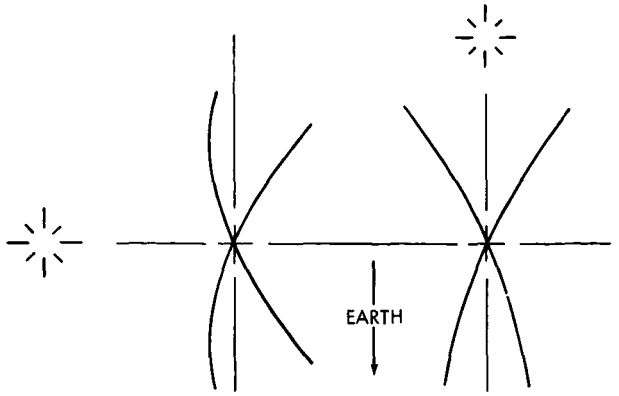

Figure 22—Solar effects on an array of booms.

of the coordinate axes, symmetry about that axis is maintained (Figure 22), but, in general, solar effects completely destroy the symmetry of the array.

Typical shapes for the array which has the parameters given above are shown in Figure 23. The equilibrium shape obtained in the absence of solar effects is shown in Figure 23a. Note the significant tip deflection of about 150 feet in this case. The closing becomes more severe for lower altitudes (e.g., a 2000-foot altitude).

The equilibrium shape obtained with the sun on the y-axis and $\Delta T_{max} = 2°F$ is shown in Figure 23b. The results of the solar effects are apparent, but are primarily confined to a rotation of the antenna pattern by a few degrees.

The critical nature of ΔT_{max} is better illustrated in Figure 23c where ΔT_{max} has been increased to 4°F and distortion of the array is much worse. Note that when the sun is on the y-axis the inward and outward looking antennas remain basically the same but are rotated out of line.

Figures 23d and 23e show the same configuration with the sun now on the x-axis and with ΔT_{max} equal to 2°F and 4°F, respectively. The effect is of an opening of the upper, and a closing of the lower, "V". This means that the two antennas now have different characteristics, although they remain in line.

Intermediate sun angles will generally result in two different basic antennas which are misaligned, and data reduction becomes complicated.

(Manuscript received June 10, 1965)

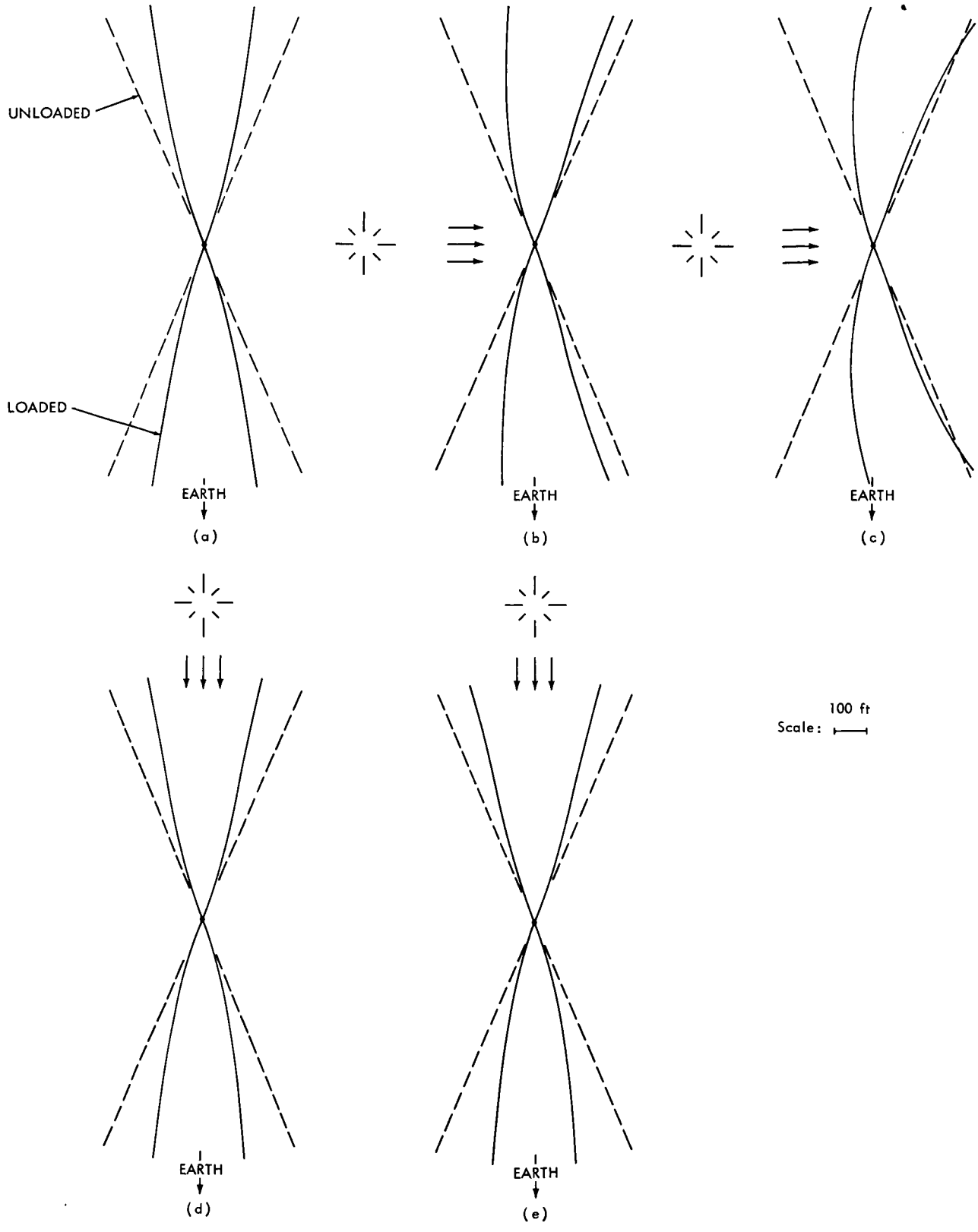

Figure 23—Equilibrium shape of array with boom length of 750 feet and V half angle of 22.5° at an altitude of 6000 km. (a) No solar effects. (b) Sun on y-axis; ΔT_{max} = 2°F. (c) Sun on y-axis; ΔT_{max} = 4°F. (d) Sun on x-axis; ΔT_{max} = 2°F. (e) Sun on x-axis; ΔT_{max} = 4°F.

Appendix A

Linear Beam Analysis

The mechanical loading on the beam consists of two components, W_{sp} which is normal to the surface and given by Equation 12, and W_{gg}, which is parallel to the x-axis and given by Equation 20.

In the linear beam analysis, the ξ, η coordinate system shown in Figure A1 is used, the loading based on the undeflected shape is calculated, and the familiar linear beam equation, modified to include thermal bending is employed. Thus,

$$\frac{d^2\eta}{d\xi^2} = -\frac{M}{EI} - \frac{e\,\Delta T_{max}}{d}\sin(\alpha-\theta) \qquad \text{(A1)}$$

with

$$\eta(0) = \frac{d\eta}{d\xi}(0) = 0 .$$

In the present case the bending moment can be written explicitly as (see Figure A2),

$$M(\xi) = \int_{\xi}^{\ell} \left(W_{sp} + W_{gg}\sin\theta\right)(\sigma-\xi)\,d\sigma , \qquad \text{(A2)}$$

where

$$W_{sp} = \frac{4}{3}p_o\, d \sin(\alpha-\theta)\,|\sin(\alpha-\theta)| ,$$

$$W_{gg} = 3\rho\omega^2\sigma\cos\theta ,$$

and

σ = dummy variable .

Thus

$$M = \int_{\xi}^{\ell} (A + B\sigma)(\sigma-\xi)\,d\sigma , \qquad \text{(A3)}$$

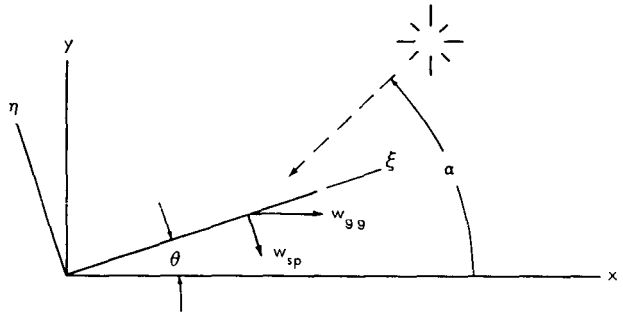

Figure A1—Coordinate system ξ, η employed in linear beam analysis.

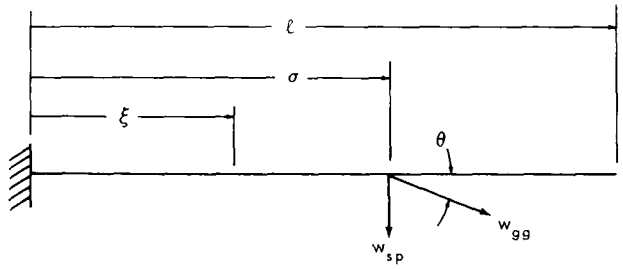

Figure A2—Simplified sketch of beam under loading.

where

$$A = \frac{4}{3} p_o d \sin(\alpha - \theta) \left| \sin(\alpha - \theta) \right| ,$$

and

$$B = \frac{3}{2} \rho \omega^2 \sin 2\theta .$$

Therefore,

$$M = A\left[\frac{\sigma^2}{2} - \xi\sigma\right]_\xi^\ell + B\left[\frac{\sigma^3}{3} - \xi\frac{\sigma^2}{2}\right]_\xi^\ell ,$$

$$= A\left(\frac{\ell^2}{2} - \ell\xi + \frac{\xi^2}{2}\right) + B\left(\frac{\ell^3}{3} - \frac{\ell^2}{2}\xi + \frac{\xi^3}{6}\right) . \qquad \text{(A4)}$$

Now,

$$\frac{d^2\eta}{d\xi^2} = -\frac{A}{EI}\left(\frac{\ell^2}{2} - \ell\xi + \frac{\xi^2}{2}\right) - \frac{B}{EI}\left(\frac{\ell^3}{3} - \frac{\ell^2}{2}\xi + \frac{\xi^3}{6}\right) - C \qquad \text{(A5)}$$

where

$$C = \frac{e\,\Delta T_{max}}{d} \sin(\alpha - \theta) .$$

Therefore,

$$\frac{d\eta}{d\xi} = -\frac{A}{EI}\left(\frac{\ell^2}{2}\xi - \frac{\ell}{2}\xi^2 + \frac{\xi^3}{6}\right) - \frac{B}{EI}\left(\frac{\ell^3}{3}\xi - \frac{\ell^2}{4}\xi^2 + \frac{\xi^4}{24}\right) - C\xi , \qquad \text{(A6)}$$

$$\eta = -\frac{A}{EI}\left(\frac{\ell^2}{4}\xi^2 - \frac{\ell}{6}\xi^3 + \frac{\xi^4}{24}\right) - \frac{B}{EI}\left(\frac{\ell^3}{6}\xi^2 - \frac{\ell^2}{12}\xi^3 + \frac{\xi^5}{120}\right) - \frac{C}{2}\xi^2 , \qquad \text{(A7)}$$

and

$$\eta(\ell) = -\frac{A\ell^4}{8EI} - \frac{11B\ell^5}{120EI} - \frac{C\ell^2}{2} . \qquad \text{(A8)}$$

The parameters listed previously can now be inserted; that is,

Length = ℓ = 750 feet,

"V" half angle = θ = 22.5°, and

Orbital altitude = 6000 kilometers.

The only required quantity not known is ω^2, and this can be found from the circular orbit condition given by

$$(R_E + h)\omega^2 = 9.8 \times 10^{-3} \frac{km}{sec^2} \left(\frac{R_E}{R_E + h}\right)^2 , \tag{A9}$$

where R_E is the radius of the earth (6378 km) and h is the orbital altitude. When h = 6000 kilometers, $\omega^2 = 2.1 \times 10^{-7}$ sec^{-2}.

If α = 90°, the constant associated with the solar pressure force becomes (with $p_o = 9.5 \times 10^{-8}$ lb/ft^2),

$$A = \frac{4}{3}(9.5 \times 10^{-8})\left(\frac{1}{24}\right)\sin^2 67.5°$$

$$= 4.50 \times 10^{-9} \text{ lb/ft} ,$$

the constant associated with the "gravity gradient" loading is

$$B = \frac{3}{2}\frac{0.017}{32.16}(2.1 \times 10^{-7})(0.707) ,$$

$$= 1.18 \times 10^{-10} \text{ lb/ft}^2 ,$$

and the constant associated with the thermal bending will be

$$C = \frac{(10^{-5})(2)}{1/24} \sin 67.5°$$

$$= 4.43 \times 10^{-4} \text{ per foot} .$$

The tip deflection $\eta(\ell)$ becomes

$$\eta(\ell) = -\frac{(4.50 \times 10^{-9})(750)^4}{8(10)} - \frac{11(1.18 \times 10^{-10})(750)^5}{120(10)}$$

$$- \frac{(4.43 \times 10^{-4})(750)^2}{2} ,$$

$$= -17.8 - 256.7 - 124.6 = 399.1 \text{ feet} .$$

This is clearly twice the tip deflection found in the computer solution of this problem (Figure 23). These numbers do however provide an indication of the relative contributions of solar pressure, "gravity gradient" loading, and thermal bending to the total deflection.

"The aeronautical and space activities of the United States shall be conducted so as to contribute . . . to the expansion of human knowledge of phenomena in the atmosphere and space. The Administration shall provide for the widest practicable and appropriate dissemination of information concerning its activities and the results thereof."

—NATIONAL AERONAUTICS AND SPACE ACT OF 1958

NASA SCIENTIFIC AND TECHNICAL PUBLICATIONS

TECHNICAL REPORTS: Scientific and technical information considered important, complete, and a lasting contribution to existing knowledge.

TECHNICAL NOTES: Information less broad in scope but nevertheless of importance as a contribution to existing knowledge.

TECHNICAL MEMORANDUMS: Information receiving limited distribution because of preliminary data, security classification, or other reasons.

CONTRACTOR REPORTS: Technical information generated in connection with a NASA contract or grant and released under NASA auspices.

TECHNICAL TRANSLATIONS: Information published in a foreign language considered to merit NASA distribution in English.

TECHNICAL REPRINTS: Information derived from NASA activities and initially published in the form of journal articles.

SPECIAL PUBLICATIONS: Information derived from or of value to NASA activities but not necessarily reporting the results of individual NASA-programmed scientific efforts. Publications include conference proceedings, monographs, data compilations, handbooks, sourcebooks, and special bibliographies.

Details on the availability of these publications may be obtained from:

SCIENTIFIC AND TECHNICAL INFORMATION DIVISION

NATIONAL AERONAUTICS AND SPACE ADMINISTRATION

Washington, D.C. 20546